ACS Macro Letters

Letter

pubs.acs.org/macroletters

Post-Fabrication Placement of Arbitrary Chemical Functionality on Microphase-Separated Thin Films of Amine-Reactive Block Copolymers

Frank W. Speetjens, II,[†,∥] Matthew C. D. Carter,[†,∥] Myungwoong Kim,[‡] Padma Gopalan,*[,†,‡] Mahesh K. Mahanthappa,*[,†,§] and David M. Lynn*[,†,§]

[†]Department of Chemistry, University of Wisconsin—Madison, 1101 University Avenue, Madison, Wisconsin 53706, United States

[‡]Department of Materials Science and Engineering, University of Wisconsin—Madison, 1509 University Avenue, Madison, Wisconsin 53706, United States

[§]Department of Chemical & Biological Engineering, University of Wisconsin—Madison, 1415 Engineering Drive, Madison, Wisconsin 53706, United States

Supporting Information

ABSTRACT: We report an approach to the post-fabrication placement of chemical functionality on microphase-separated thin films of a reactive block copolymer. Our approach makes use of an azlactone-containing block copolymer that microphase separates into domains of perpendicularly-oriented lamellae. These thin films present nanoscale patterns of amine-reactive groups (reactive stripes) that serve as handles for the immobilization of primary amine-containing functionality. We demonstrate that arbitrary chemical functionality can be installed by treatment with aqueous solutions under mild conditions that do not perturb underlying microphase-separated patterns dictated by the structure of the reactive block copolymer. This post-fabrication approach provides a basis for the development of modular approaches to the design of microphase-separated block copolymer thin films and access to coatings with patterned chemical domains and surface properties that would be difficult to prepare by the self-assembly and processing of functionally complex block copolymers.

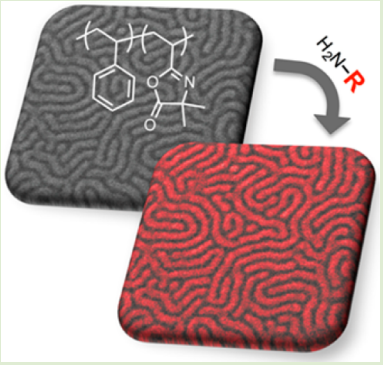

Block copolymers (BCPs) that microphase separate into periodic domains provide powerful opportunities to define the nanoscale structures, bulk properties, and interfacial behaviors of soft materials.[1−3] Due to the molecular length scales at which they microphase separate, BCP thin films that exhibit lamellar or cylindrical morphologies are of particular technological interest and can provide precise, nanoscale control over the placement and patterning of chemical functionality on film-coated surfaces.[4−7] This feature of BCP thin films has been exploited fruitfully to develop new approaches to advanced lithography and create well-defined, periodic patterns of chemical and biological groups on surfaces relevant to the design of nano/biointerfaces, substrates for the directed growth, deposition, or capture of nanoparticles and other emerging applications.[8−13]

Much is now understood about the influence of polymer structure on the microphase separation of BCPs.[1,5] In principle, one might envision exploiting that understanding to design new BCPs that could direct the periodic placement or presentation of arbitrary functionality on the surface or within the bulk of a substrate-supported film (e.g., in alternating lamellar stripes or as arrays of functional "spots" created by cylindrical morphologies). Unfortunately, however, the individual blocks of a given BCP cannot simply be "swapped out" for others without perturbing key parameters that define the morphology of the original copolymer and its behavior in thin films.[1−3,14] In general, it remains difficult to predict the effects of introducing arbitrary and structurally complex chemical features on BCP phase behavior because of the sensitivity of microphase separation to small structural variations.

The bulk microphase separation of a polymer comprised of two chemically distinct blocks (a diblock copolymer) is governed by both the relative volume fractions of each block ($f_A = 1 - f_B$) and the segregation strength ($\chi_{AB}N$) that quantifies the mutual block repulsion energy that drives structure formation.[1−5] While theoretical and experimental studies have established relationships between the values of these order parameters and observed bulk microphase separation behavior,[1,5] small changes to the structure of one block (e.g., a change in side chain structure) can lead to significant changes in morphology and nano-domain periodicity.[1−5,14,15] The use of BCP thin films in several applied contexts also depends crucially on controlling interfacially confined morphologies and their preferred orientations relative to underlying substrates, both of which depend sensitively on film thickness and the relative surface energies of each

Received: October 17, 2014
Accepted: October 20, 2014
Published: October 27, 2014

   dx.doi.org/10.1021/mz500654a | ACS Macro Lett. 2014, 3, 1178−1182

block.[4−13,16] For these and other reasons, exerting predictable and universal control over the microphase separation of BCP thin films in a manner that is independent of specific polymer structure and other processing parameters remains a substantial fundamental challenge.

The sensitive dependence of microphase separation on BCP structure makes it difficult to develop modular and general approaches to the design of well-defined BCP interfaces. Although it is now straightforward to synthesize libraries of otherwise identical AB diblocks with B blocks containing different side chain functionalities, the thin film phase behaviors of these materials would likely vary widely and be difficult to predict. Even if the interfacial properties of these BCPs permitted uniform film fabrication (e.g., no de-wetting), those films would likely exhibit a range of microphase-separated or disordered morphologies (with orientations that vary relative to the substrate) that present B-block functionality in substantially different locations on the surface or in the bulk. Here, we report an approach to the fabrication of reactive microphase-separated BCP thin films that side-steps these fundamental issues and permits systematic, post-fabrication installation of arbitrary functionality on well-defined microphase-separated coatings.

Our approach makes use of azlactone-containing BCPs that microphase separate into domains of perpendicularly oriented lamellae. These films present nanoscale patterns of surface-exposed amine-reactive groups (reactive stripes) that serve as "handles" for the subsequent immobilization of arbitrary chemical functionality. This post-fabrication approach circumvents problems associated with the influence of polymer structure on BCP phase behavior and affords microphase-separated coatings that can be used to vary the features presented by alternating lamellar domains over a broad range of structural and functional space. This strategy thus provides a basis for the development of "universal" approaches to the interfacial engineering of microphase-separated BCP thin films and, thereby, access to coatings with patterned chemical domains and surface properties (e.g., wetting behaviors, binding affinities, etc.) that would be difficult to prepare by the self-assembly of functionally complex BCPs. Our results demonstrate proof-of-concept using a model amine-reactive BCP and provide guiding principles for the design of well-defined soft matter interfaces of interest in many fundamental and applied contexts.

We selected diblock copolymers with one block containing azlactone groups for use in this study for several reasons: (i) azlactones react through ring-opening reactions with a broad range of nucleophiles,[17] (ii) reactions with primary amines occur rapidly to produce stable amide bonds under mild conditions, without the need for a catalyst or the generation of byproducts,[17] (iii) azlactones are stable under typical BCP thermal processing conditions,[18] and (iv) vinyl azlactones can be copolymerized with other vinyl monomers using living/controlled methods to produce reactive BCPs with a range of side chain functionalities.[18−23] Relative to past approaches to the fabrication of oriented thin films of reactive BCPs,[24−27] this approach introduces several practical advantages. While past studies have reported solution-phase characterization of azlactone-functionalized BCPs,[22,23,28,29] investigations of the bulk and thin film phase behaviors of these reactive copolymers are limited.[18] Our results provide insight into the solid-state structures and morphologies of these reactive materials and demonstrate proof-of-concept with respect to selective functionalization of reactive domains in microphase-separated lamellar thin films. In this work, we used a model diblock copolymer synthesized by RAFT polymerization of styrene (S) and 2-vinyl-4,4-dimethylazlactone (VDMA; Figure 1).

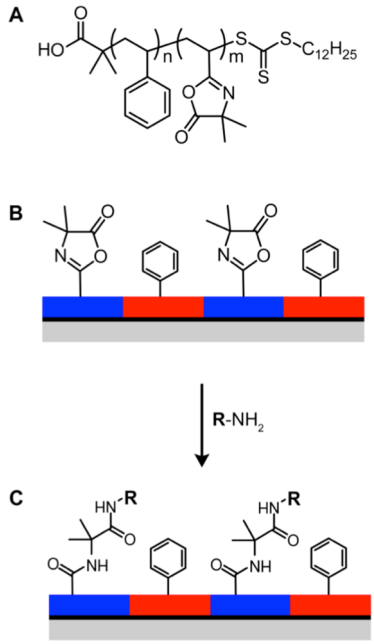

Figure 1. (A) Structure of PS-*b*-PVDMA. (B) Cross-section of a PS-*b*-PVDMA thin film microphase separated into perpendicular lamellae with alternating, surface-exposed stripes of PVDMA segments (blue) and non-reactive PS segments (red). (C) Selective ring-opening of azlactone groups in reactive stripes (blue) by treatment with primary amines permits placement of secondary functionality in defined locations without disrupting the underlying nanoscale morphology.

Polymerization of styrene was performed using *S*-1-dodecyl-*S*′-(α,α′-dimethyl-α″-acetic acid)trithiocarbonate as a chain transfer agent to produce a PS macromolecular chain transfer agent (M_n = 15.7 kg/mol, $Đ$ = 1.16), followed by chain extension with VDMA to produce PS-*b*-PVDMA (M_n = 33.6 kg/mol, $Đ$ = 1.33) with blocks of roughly equal molecular weights (see Scheme S1A, Figure S1, and Methods in the Supporting Information for details of synthesis and characterization). DSC revealed a single thermal transition at 111 °C, associated with the T_g of both the PS and PVDMA homopolymer segments (Figure S2, Supporting Information); thermogravimetric analysis revealed a mass loss of <5% at temperatures up to 248 °C (Figure S3, Supporting Information). This result permitted characterization of bulk samples of PS-*b*-PVDMA by small-angle X-ray scattering (SAXS) at temperatures above the T_g of the material without inducing thermal degradation. SAXS traces acquired at 150 °C (Figure 2, red curve) revealed a sharp principal scattering peak at q^* = 0.0209 Å^{-1} with higher-order reflections at $q/q^* = \sqrt{4}$, $\sqrt{9}$, $\sqrt{16}$, and $\sqrt{25}$ (a high-resolution synchrotron SAXS pattern is provided in Figure S4, Supporting Information). On the basis of the positions of these peaks, coupled with the diminished intensity of the $\sqrt{4}$ peak, we conclude that this copolymer assembles into a bulk lamellar morphology with roughly symmetric volume fractions of each block and a lamellar spacing L_0 = 30.1 nm. We return to Figure 2 and the influence of side chain substitution on the bulk phase behavior of this reactive BCP in the discussion below.

dx.doi.org/10.1021/mz500654a | *ACS Macro Lett.* 2014, 3, 1178−1182

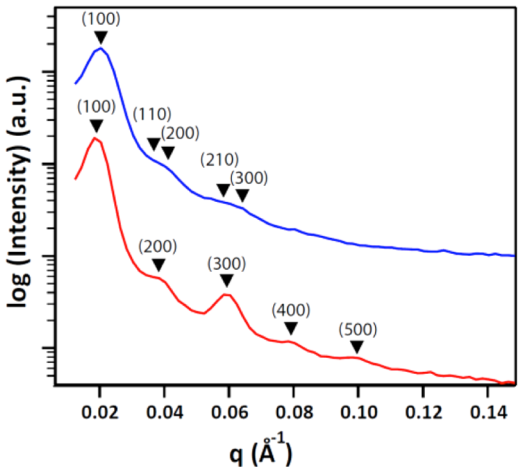

Figure 2. Azimuthally-integrated SAXS patterns for PS-*b*-PVDMA (red) and the product of exhaustive reaction of PS-*b*-PVDMA with dimethylaminopropylamine (blue), after thermal annealing at 150 °C. The peak markers for PS-*b*-PVDMA correspond to the calculated peak positions of a lamellar morphology, with a principal scattering wavevector q^* = 0.0209 Å^{-1}. Functionalization with dimethylaminopropylamine causes the resulting block copolymer to microphase separate into hexagonally packed cylinders with q^* = 0.0213 Å^{-1}, as indicated by peak markers corresponding to the calculated positions of expected reflections.

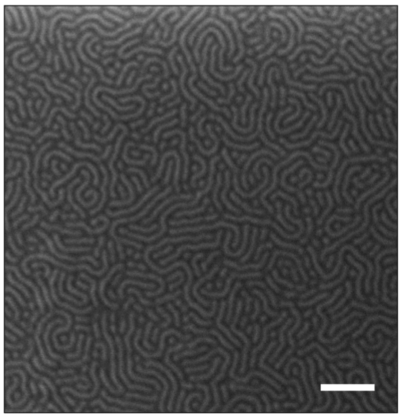

Figure 3. SEM image of a perpendicularly-oriented lamellar thin film obtained by spin-coating and thermal annealing of PS-*b*-PVDMA at 160 °C on a neutral mat composed of poly(styrene-*r*-methyl methacrylate-*r*-glycidyl methacrylate) with a styrene mole fraction of 0.43. Scale = 200 nm. Films exhibited uniformity across the substrate and no indication of dewetting over large areas (see Figure S6 in the Supporting Information).

Figure 3 shows a representative SEM image of a thin film of PS-*b*-PVDMA spin-coated and annealed on a silicon substrate coated with a poly(styrene-*r*-methyl methacrylate-*r*-glycidyl methacrylate) cross-linked copolymer mat.[4,30] For this and all other studies below, we used a mat composition with a mole fraction of styrene, F_S, of 0.43 determined from ^{1}H NMR. Films of PS-*b*-PVDMA 22 nm thick ($0.73L_0$) were cast on these mats by spin-coating, and samples were then thermally annealed at 160 °C for 4 h at 1 Torr. Figure 3 reveals a microphase-separated pattern with characteristics of a perpendicularly oriented lamellar BCP,[4,8,13,30] as anticipated from the SAXS analyses above (Figure 2, red curve; see also Figure S6 (Supporting Information) for additional SEM images). The nanodomain periodicity from SEM is also consistent with the domain spacing of the bulk lamellar morphology measured by SAXS ($L_0 \sim 30$ nm; Figure S5, Supporting Information). It is not possible to assign the specific locations of the S and VDMA blocks solely on the basis of these SEM images. However, we interpret the regions of light and dark contrast in Figure 3 to represent alternating nanoscale stripes of PS and reactive PVDMA blocks. Characterization by infrared reflection absorption spectroscopy confirmed that the azlactone groups of the copolymer remained intact and were not hydrolyzed or degraded by thermal annealing (e.g., as revealed by stretches at 1830, 1679, and 1209 cm^{-1} associated with the C═O, C═N, and C−O−C bonds of the azlactone ring; see Figure S7, Supporting Information).

Further studies demonstrated that the azlactones in thermally annealed PS-*b*-PVDMA films were surface-accessible and that reactive lamellae could be used to introduce secondary functionality and tailor interfacial properties without compromising underlying phase-separated domains. The images in Figure 4A,C show micrographs of thermally annealed films treated with aqueous solutions of either (A) a primary amine-functionalized fluorophore (tetramethylrhodamine cadaverine; TMR-cad) or (C) a non-reactive (amine-free) analogue (tetramethylrhodamine; TMR) for 20 min at ambient temperature. These images reveal uniform red fluorescence on the film treated with TMR-cad relative to the film treated with TMR. These results reveal non-specific physisorption of TMR to be negligible, suggesting that fluorescence observed in Figure 4A arises solely from the reaction of TMR-cad with the azlactone groups of PVDMA (Figure 1B,C).

We used water as a medium for the experiments above because it is a non-solvent for both PS and PVDMA homopolymers and should, thus, prevent lamellar domain reorientation or disruption that could arise from use of organic solvents. Figure 4B,D shows SEM images of the same films shown in Figure 4A,C after treatment with aqueous solutions of TMR or TMR-cad. The morphologies of the treated films are similar to those of the films prior to treatment (cf. Figure 3), leading us to conclude that these mild conditions do not substantially reorganize the underlying morphology. These images also illustrate how new and complex chemical functionality—here, a large and positively charged fluorophore—can be introduced to a self-assembled BCP film without disturbing the original phase arising from the reactive parent copolymer. Given the absence of observed physisorption, we infer that functionalization occurs selectively on lamellar stripes defined by the PVDMA domains.

The features of this reactive BCP platform are significant in several contexts. First, they enable the selective, post-fabrication placement of new chemical functionality on the surfaces of BCP thin films in domains with shapes, sizes, and characteristic length scales that can be precisely defined by the structure of the reactive parent copolymer. Provided that mild chemical functionalization can be achieved using methods and reagents that do not perturb the film morphology, this approach provides opportunities to create well-defined and functional BCP interfaces in which the chemical functionality of one domain can be varied systematically and orthogonally to all other physical and microstructural features. This approach thus circumvents issues associated with the dependence of BCP phase behavior on chemical structure by using a "noninvasive" approach to introduce new functionality after the microphase-separated morphology has been fixed by vitrification of the glassy PS domains. Finally, we note that this post-fabrication

dx.doi.org/10.1021/mz500654a | *ACS Macro Lett.* 2014, 3, 1178−1182

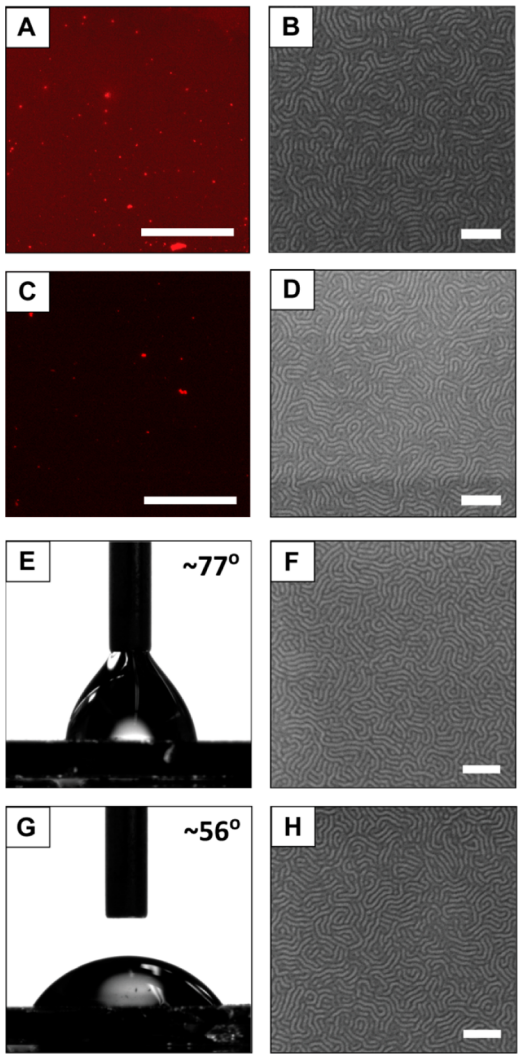

Figure 4. (A–D) Fluorescence micrographs and SEM images of PS-*b*-PVDMA films acquired after treatment with aqueous solutions of (A,B) TMR-cad or (C,D) TMR. The absence of fluorescence in (C) suggests negligible non-specific physisorption and that fluorescence in (A) arises from the reaction of TMR-cad with the azlactone groups in PS-*b*-PVDMA; scale bars in (A) and (C) are 125 μm. (E–H) Advancing (E) and static (G) contact angles and SEM images for thin films after treatment with (E,F) propylamine or (G,H) dimethylaminopropylamine. Scale for SEM images = 200 nm. SEM images show that domain orientation is retained post-functionalization.

approach to functionalization opens the door to the placement of complex chemical or biological functionality on the surfaces of microphase-separated thin films in a manner that would be difficult to achieve by either thermal or solvent annealing of functional BCPs (due to the potentially problematic thermal stabilities of more complex functional groups or the interfacial wetting behaviors of these materials).

The results described above provide opportunities to introduce chemical or biological functionality to reactive lamellar domains using a diverse pool of water-soluble primary amines. The images in Figure 4E,G show water contact angles (θ) for lamellar PS-*b*-PVDMA films treated with aqueous solutions of either (E) the hydrophobic amine propylamine or (G) the hydrophilic amine dimethylaminopropylamine (SEM images in Figure 4F,H show that morphology is retained after functionalization). These images reveal films treated with propylamine to be hydrophobic (θ_{adv} = 77.0 ± 1.5°); films treated with dimethylaminopropylamine were significantly more hydrophilic (θ_{stat} = 55.8 ± 2.3°). These differences are consistent with differences in the hydrophobicity and hydrophilicity of these amines. These results provide additional support for the reactivity of these microphase-separated films with amines of arbitrary structure and provide principles useful for modifying the interfacial behaviors of BCP thin films. This approach should prove useful for the immobilization and patterning of a range of other chemical and biological functionality. The identification of other solvent systems that do not dissolve PS-*b*-PVDMA or perturb underlying BCP domain structures would also further broaden the range of amines that can be used to functionalize or tune the properties of these materials.

Finally, we return to Figure 2 (blue curve), which depicts the SAXS pattern of a BCP synthesized by solution-phase treatment of PS-*b*-PVDMA with an excess of dimethylaminopropylamine (used to prepare the hydrophilic coatings described above; Figure 4G,H) to install dimethylaminopropyl side chains on the PVDMA block (>95% functionalized; see Figure S8 and Scheme S1B, Supporting Information, for details). The SAXS trace of this BCP at 150 °C (above the T_g of both homopolymer segments; Figure S9, Supporting Information) showed a principal peak at q^* = 0.0213 Å^{-1} (L_0 = 29.5 nm) and higher-order reflections at q/q^* = $\sqrt{3}$, $\sqrt{4}$, $\sqrt{7}$, and $\sqrt{9}$. On the basis of these relative peak positions, we conclude that this functionalized BCP assembles into hexagonally close-packed cylinders in the bulk, a morphology that differs substantially from the lamellar morphology of the reactive PS-*b*-PVDMA template from which it was synthesized (Figure 2, red curve). While this difference in morphology is not particularly surprising, it underscores the impact that changes in block structure can have on the resulting microphase-separated morphologies of BCPs. This result thus highlights the versatility and potential utility of the post-functionalization approach reported here, as it would likely prove difficult to anneal a pre-synthesized BCP with segments bearing styryl and dimethylamino groups into the lamellar thin films that we readily fabricated through our post-fabrication functionalization approach.

Approaches to the design of soft material interfaces that enable precise control over the presentation of chemically and biologically relevant functionalities on surfaces provide opportunities to design nano/biointerfaces for advanced applications. While BCP thin film self-assembly presents a promising path toward these goals, it is intrinsically limited by the fact that copolymer self-assembly and processability are sensitive to the chemical compositions of BCPs. We have described an approach that side-steps this limitation by exploiting the self-assembly of a PS-based diblock copolymer with a second amine-reactive block. This reactive BCP microphase separates into a lamellar thin film morphology, with a preferential perpendicular domain orientation relative to underlying substrates. This morphology provides periodic, nanoscale stripes of azlactone-functionalized segments that can be functionalized, post-fabrication, by treatment with aqueous solutions of primary amines. Because vitreous PS domains cement the film structure, this approach leads to periodic arrays presenting new functionality without disturbing the morphology or domain orientation of the coating. This approach is modular, in terms of both the range of amine-functionalized motifs that can be installed and the variety of vinyl monomers

dx.doi.org/10.1021/mz500654a | *ACS Macro Lett.* 2014, 3, 1178–1182

that can be copolymerized with VDMA. We anticipate that this approach can be extended to the design of films that assemble into other reactive morphologies (e.g., perpendicular cylinders, aligned lamellae, or features with domain spacings smaller than those reported here) by judicious choice of polymer structure and careful design of underlying substrates.

■ ASSOCIATED CONTENT

Supporting Information

A detailed description of experimental procedures and supporting figures. This material is available free of charge via the Internet at http://pubs.acs.org.

■ AUTHOR INFORMATION

Corresponding Authors

*Prof. Padma Gopalan. E-mail: pgopalan@cae.wisc.edu.
*Prof. Mahesh K. Mahanthappa. E-mail: mahesh@chem.wisc.edu.
*Prof. David M. Lynn. E-mail: dlynn@engr.wisc.edu.

Author Contributions

‖These authors contributed equally.

Notes

The authors declare no competing financial interest.

■ ACKNOWLEDGMENTS

This work was supported by the NSF through a grant to the Nanoscale Science and Engineering Center at UW-Madison (DMR-0832760) and made use of NSF-supported facilities (DMR-0832760, DMR-1121288, and CHE-1048642). Synchrotron SAXS studies were conducted at Sector 12 of the Advanced Photon Source at Argonne National Laboratory, supported by the U.S. DOE (Contract #DE-AC02-06CH11357). M.C.D.C. acknowledges the Natural Sciences Engineering Research Council of Canada for a graduate fellowship.

■ REFERENCES

(1) Bates, F. S.; Fredrickson, G. H. *Phys. Today* **1999**, *52*, 32.
(2) Lodge, T. P. *Macromol. Chem. Phys.* **2003**, *204*, 265.
(3) Ruzette, A.-V.; Leibler, L. *Nat. Mater.* **2005**, *4*, 19.
(4) Bang, J.; Jeong, U.; Ryu, D. Y.; Russell, T. P.; Hawker, C. J. *Adv. Mater.* **2009**, *21*, 4769.
(5) Marencic, A. P.; Register, R. A. *Annu. Rev. Chem. Biomol. Eng.* **2010**, *1*, 277.
(6) Luo, M.; Epps, T. H., III *Macromolecules* **2013**, *46*, 7567.
(7) Hu, H.; Gopinadhan, M.; Osuji, C. O. *Soft Matter* **2014**, *10*, 3867.
(8) Kim, S. O.; Solak, H. H.; Stoykovich, M. P.; Ferrier, N. J.; de Pablo, J. J.; Nealey, P. F. *Nature* **2003**, *424*, 411.
(9) Tang, C. B.; Lennon, E. M.; Fredrickson, G. H.; Kramer, E. J.; Hawker, C. J. *Science* **2008**, *322*, 429.
(10) Peng, Q.; Tseng, Y.-C.; Darling, S. B.; Elam, J. W. *Adv. Mater.* **2010**, *22*, 5129.
(11) Xu, J.; Hong, S. W.; Gu, W.; Lee, K. Y.; Kuo, D. S.; Xiao, S.; Russell, T. P. *Adv. Mater.* **2011**, *23*, 5755.
(12) Killops, K. L.; Gupta, N.; Dimitriou, M. D.; Lynd, N. A.; Jung, H.; Tran, H.; Bang, J.; Campos, L. M. *ACS Macro Lett.* **2012**, *1*, 758.
(13) Bates, C. M.; Seshimo, T.; Maher, M. J.; Durand, W. J.; Cushen, J. D.; Dean, L. M.; Blachut, G.; Ellison, C. J.; Willson, C. G. *Science* **2012**, *338*, 775.
(14) Cochran, E. W.; Bates, F. S. *Macromolecules* **2002**, *35*, 7368.
(15) Kennemur, J. G.; Hillmyer, M. A.; Bates, F. S. *Macromolecules* **2012**, *45*, 7228.
(16) Stein, G. E.; Mahadevapuram, N.; Mitra, I. *J. Polym. Sci., Part B: Polym. Phys.* **2014**, DOI: 10.1002/polb.23502.
(17) Heilmann, S. M.; Rasmussen, J. K.; Krepski, L. R. *J. Polym. Sci., Part A: Polym. Chem.* **2001**, *39*, 3655.
(18) Lokitz, B. S.; Wei, J.; Hinestrosa, J. P.; Ivanov, I.; Browning, J. F.; Ankner, J. F.; Kilbey, S. M.; Messman, J. M. *Macromolecules* **2012**, *45*, 6438.
(19) Tully, D. C.; Roberts, M. J.; Geierstanger, B. H.; Grubbs, R. B. *Macromolecules* **2003**, *36*, 4302.
(20) Fournier, D.; Pascual, S.; Fontaine, L. *Macromolecules* **2004**, *37*, 330.
(21) Pascual, S.; Blin, T.; Saikia, P. J.; Thomas, M.; Gosselin, P.; Fontaine, L. *J. Polym. Sci., Part A: Polym. Chem.* **2010**, *48*, 5053.
(22) Buck, M. E.; Lynn, D. M. *Polym. Chem.* **2012**, *3*, 66.
(23) Ho, H. T.; Levere, M. E.; Fournier, D.; Montembault, V.; Pascual, S.; Fontaine, L. *Aust. J. Chem.* **2012**, *65*, 970.
(24) Shen, L.; Garland, A.; Wang, Y.; Li, Z.; Bielawski, C. W.; Guo, A.; Zhu, X. Y. *Small* **2012**, *8*, 3169.
(25) Stadermann, J.; Riedel, M.; Komber, H.; Simon, F.; Voit, B. *J. Polym. Sci., Part A: Polym. Chem.* **2012**, *50*, 1351.
(26) Zhao, H.; Gu, W.; Kakuchi, R.; Sun, Z.; Sterner, E.; Russell, T. P.; Coughlin, E. B.; Theato, P. *ACS Macro Lett.* **2013**, *2*, 966.
(27) Zhao, H.; Gu, W.; Thielke, M. W.; Sterner, E.; Tsai, T.; Russell, T. P.; Coughlin, E. B.; Theato, P. *Macromolecules* **2013**, *46*, 5195.
(28) Quek, J. Y.; Zhu, Y.; Roth, P. J.; Davis, T. P.; Lowe, A. B. *Macromolecules* **2013**, *46*, 7290.
(29) Ho, H. T.; Levere, M. E.; Pascual, S.; Montembault, V.; Casse, N.; Caruso, A.; Fontaine, L. *Polym. Chem.* **2013**, *4*, 675.
(30) Han, E.; Gopalan, P. *Langmuir* **2010**, *26*, 1311.